Two-Stream Effects in Present and Future Accelerators

F. Zimmermann, CERN, Geneva, Switzerland

Abstract

Electron beams are perturbed by ions in a similar way as proton and positron beams are by electrons, generated via gas ionization, photoemission, or multipacting. Fast beam-ion or electron-cloud 'two-stream' instabilities become more severe for higher beam current or closer bunch spacing, and they may limit the ultimate performance of an accelerator. For the Large Hadron Collider (LHC), the heat load deposited by electrons on the beam screen inside the superconducting magnets is a concern. I compare theories and simulations of these 'two-stream' effects with observations at various storage rings, e.g., ALS, PLS, SPS, and KEKB, and comment on future machines, such as the LHC, the damping rings of a future linear collider, and a possible LHC upgrade operating with long 'superbunches'.

1 INTRODUCTION

In the design of modern accelerators, conventional beam instabilities appear well under control. They are either avoided by a careful optimization of the impedance or suppressed by fast feedback systems. Relying on this strategy, present and future projects aim to increase the beam currents and the number of bunches by orders of magnitude, *e.g.*, the LHC, the B and super-B factories, or some high-intensity proton machines, and to reduce the emittances to unprecedentedly small values, *e.g.*, light sources, X-ray FELs, and linear colliders. The ultimate performance of these machines will likely be limited by two-stream effects, namely by the interaction of a charged particle beam with a second particle species, usually of opposite charge, which can cause emittance growth and fast instabilities that cannot be cured by a conventional feedback. The two most prominent two-stream effects in present accelerators are the fast beam-ion instability (FBII) [1, 2], which is experienced by electron or negatively charged ion beams even in the presence of an ion clearing gap, and the electron-cloud instability (ECI) [3, 4, 5, 6], which occurs for proton, positron and positively charged ion beams consisting of many closely spaced bunches or a single long bunch. These two instabilities are conceptually similar; in both cases the motion of ions or electrons strongly amplifies an initial perturbation in the beam. While the FBII is usually a coupled bunch instability, the ECI can be of both the coupled-bunch or single-bunch type. Observations and general theory of FBII and ECI have been discussed in several recent papers [7, 8, 9] and workshop proceedings [10, 11].

2 FAST BEAM-ION INSTABILITY

A charged particle beam ionizes the residual gas. The ions are produced at a rate

$$\dot{\lambda}_{\rm ion}[{\rm m}^{-1}{\rm s}^{-1}] = (I_{\rm beam}/q)\sigma_{\rm ion}d_{\rm gas} \qquad (1)$$

where $d_{\rm gas}$ is the molecule density in ${\rm m}^{-3}$, $\lambda_{\rm ion}$ the ion line density in ${\rm m}^{-1}$, $I_{\rm beam}$ the beam current, and q the beam-particle charge. At relativistic energies the ionization cross section $\sigma_{\rm ion}$ is about 2 Mbarn, for carbon monoxide. Ions can also be produced via residual-gas ionization or desorption by synchrotron radiation or via beam loss. The number of ions created by synchrotron radiation may exceed that from beam-gas ionization by a factor $(\sigma^\gamma_{\rm ion}/\sigma_{\rm ion})(5/(2\sqrt{3})\gamma/137)\sqrt{2h_x/\rho}$, where h_x denotes the half width of the chamber, γ the Lorentz factor, $\sigma^\gamma_{\rm ion}$ the photoionization cross section at typical photon energies. For photon energies below 100 eV and carbon monoxide, $\sigma^\gamma_{\rm ion}$ is 5–20 Mbarn.

A negatively charged beam attracts the positively charged ions. We consider a beam of n_b bunches, uniformly distributed around the ring circumference C and each containing N_b electrons. The transverse rms beam sizes are denoted by σ_x and σ_y, and the bunch spacing by $L_{\rm sep} = C/n_b$. For small $L_{\rm sep}$, the ions are trapped near the beam axis, where they experience an almost linear restoring force from each passing bunch, and perform quasi-harmonic transverse oscillations around the beam center. Their horizontal and vertical angular oscillation frequencies are

$$\omega_{i;x,y} \approx \left(\frac{2N_b n_b r_p Q c^2}{C\sigma_{x,y}(\sigma_x+\sigma_y)A}\right)^{1/2}, \qquad (2)$$

where c denotes the speed of light, r_p denotes the classical proton radius, A the ion mass in units of the proton mass m_p, and Q the ion charge in units of the electron charge e. In electron rings, the vertical rms beam size σ_y is usually smaller than the horizontal rms size σ_x, and, therefore, the vertical ion frequency is larger than the horizontal one. In this case, the ion trapping condition is $\omega_{i;y}L_{\rm sep}/c \ll 2$.

If ions survive and accumulate in the beam potential over successive turns, they can induce a 'classical' trapped ion instability, which has been observed since decades at many storage rings [12]. In order to avoid this type of instability, most accelerators introduce a clearing gap in the bunch train. The duration of the gap should be much larger than the ion oscillation period, or $t_{\rm gap} \gg 1/\omega_{i;y}$.

If a clearing gap removes the ions, the maximum number of ions is limited to those produced during a single passage of the bunch train. However, modern factories and future collider projects require much higher beam current than previous storage rings, and the ion production rate (1) increases correspondingly. In addition, high-quality beams are characterized by small beam sizes, implying a strong force acting between the beam and the ions. Therefore, in 1994 it was predicted that an ion instability similar to multi-bunch beam break up in a linac, namely the FBII,

can occur even in the presence of a clearing gap. In this case, the coupling strength between beam and ions is not a constant but, due to the ion production, it increases linearly along the bunch train. We write $K = \dot{K}z/c$ where z denotes the distance from the head of the bunch train (we assume a relativistic beam), and, using $\dot{\lambda}_{\rm ion}$ from (1),

$$\dot{K}_{x,y} = \frac{2\dot{\lambda}_{\rm ion} r_e c^2}{\gamma\sigma_{x,y}(\sigma_x + \sigma_y)} \; . \tag{3}$$

Without any ion frequency spread, the bunch oscillation amplitudes grow as

$$y_b(s,z) \propto \exp\left(\sqrt{\frac{s}{c\tau_{\rm FBII}}}\frac{z}{l_{\rm train}}\right), \tag{4}$$

where s denotes the position along the beam line, $l_{\rm train}$ the length of the bunch train, and the quasi-exponential instability rise time at the end of the bunch train ($z = l_{\rm train}$) is [1, 2, 14]

$$\tau_{\rm FBII} = \frac{2\omega_\beta c^2}{\dot{K}_{\rm ion}\bar{\omega}_i l_{\rm train}^2} \; , \tag{5}$$

where $\bar{\omega}_i = \sqrt{2/3}\omega_i$ is the approximate ion centroid frequency. Inserting the definitions, the growth rate can also be written as [1]

$$\frac{1}{\tau_{\rm FBII}} = \frac{4 d_{\rm gas}\sigma_{\rm ion}\beta_y N_b^2 r_e^{3/2} n_b^2 L_{\rm sep}^{1/2} c}{\sqrt{27}\gamma\sigma_y^{3/2}(\sigma_x+\sigma_y)^{3/2}A^{1/2}} \; . \tag{6}$$

The growth of unstable oscillations ceases at amplitudes comparable to the rms beam size, since here the beam-ion force becomes strongly nonlinear [15]. In addition, the variation of the beam sizes around the ring, the presence of multiple ion species, the dependence of the vertical ion frequency on the horizontal position, as well as the nonlinearity of the beam field, all introduce a spread in the ion frequency. This ion frequency spread qualitatively changes the character of the instability, so as to become truly exponential [13, 14]. For a normal distribution of ion frequencies, with mean $\bar{\omega}_i$ and standard deviation σ_ω, the amplitude grows as

$$y_b(s,z) \propto \exp\left(\frac{s}{c\tau_{\rm FBII2}}\frac{z}{l_{\rm train}}\right) \tag{7}$$

where

$$\tau_{\rm FBII2} = \frac{2\omega_\beta c}{\dot{K} l_{\rm train}}\left[\sqrt{\frac{8}{\pi}}\frac{\sigma_\omega}{\bar{\omega}_i}\right] \; . \tag{8}$$

If the ion distribution is broad, $\sigma_\omega \approx \bar{\omega}_i$, the instability growth rate equals the incoherent betatron frequency shift due to the ions $1/\tau_{\rm FBII2} \approx \Delta\omega_\beta \approx (2\omega_\beta c/(\dot{K} l_{\rm train}))$ [14].

Soon after it was first predicted [1, 2], the FBII was confirmed experimentally in a dedicated study at the Advanced Light Source (ALS) [16]. The ALS observations included an increase of the projected vertical beam size by a factor 2–3 and coherent betatron oscillation characteristic of ion induced instabilities. For this experiment, helium gas was injected to provide an elevated vacuum pressure of up to 80 nTorr, a large clearing gap prevented multiturn ion trapping, and the transverse feedback suppressed all conventional instabilities. Similar studies at the TRISTAN AR [17], and at the Pohang Light Source (PLS) [18], further validated the predictions. In the PLS experiments, a streak camera measured both an actual beam size increase by a factor 2 and bunch centroid oscillations of about $1\sigma_y$ along the train. The instability was observed for 0.16 ntorr partial pressure of carbon monoxide. These experiments demonstrated that short gaps in the bunch train, the presence of different ion species, or enlarged chromaticity may damp the instability [18, 19].

More recently, the FBII has been observed in the KEKB HER during commissioning [20]. The KEKB analysis applied a singular-value decomposition [21] to multi-turn bunch-by-bunch position data [20]. The fitted growth rate was consistent with the theoretical prediction. The instability has also been seen at the ESRF when operating with a low-emittance lattice [22] and at SPring-8 [23], after vacuum intervention. Table 1 summarizes the conditions under which the FBII was observed and the estimated rise times, which were all of the order of 1 ms. After further increases to the bunch current at KEKB, since 2001 a strong horizontal instability is seen in the HER [24]. Also here, a possible explanation is the FBII, which may manifest itself in the horizontal plane if the ions (in this case we suppose hydrogen) are overfocused between bunches vertically, but remain trapped horizontally.

The predicted exponential rise times $\tau_{\rm FBII2}$ for the damping rings of (future) linear colliders are about 1–10 μs at 1 ntorr vacuum pressure [25]. This regime may be reached in multibunch operation at the KEK/ATF [26].

3 ELECTRON CLOUD

Positively charged beams preferably interact with electrons. These can be trapped in the beam potential, just as ions are attracted by beams of negative charge. The electrons oscillate inside a single Gaussian bunch of rms length σ_z with the approximate frequency

$$\omega_{e;x,y} \approx c\left(\frac{2N_b r_e}{\sqrt{2\pi}\sigma_z\sigma_{x,y}(\sigma_x+\sigma_y)}\right)^{1/2} \; . \tag{9}$$

The electron oscillation frequency ω_e is much larger than ω_i, due to the large mass difference of ions and electrons. Electrons can, thus, more easily induce single-bunch instabilities, in addition to coupled-bunch instabilities.

In most proton rings, the dominant source of electrons is gas ionization or beam loss, in most positron rings photoemisson due to synchrotron radiation. In either case, for close bunch spacing beam-induced multipacting [28] can further amplify the number of electrons. A necessary condition for the electron amplification via multipacting is that the effective secondary emission yield exceeds 1. The latter depends on the energy gained by electrons in the beam field, and, hence, on the bunch current, the bunch length,

Table 1: Parameters for which FBII was observed in existing storage rings, and the e-folding rise time τ_e inferred from the experiment; other symbols refer to geometric emittances ($\epsilon_{x,y}$), beam energy (E),bunch spacing ($t_{\rm sep}$), average beta function, ($\beta_{x,y}$), vacuum pressure (p), number of bunches (n_b), and bunch population (N_b). A similar instability was studied in the FNAL H^- linac [27].

accelerator	ϵ_x (nm)	ϵ_y (pm)	E (GeV)	n_b	N_b (10^{10})	$t_{\rm sep}$ (ns)	$\beta_{x,y}$ (m)	p [ntorr]	τ_e (ms)
ALS [16]	4	136	1.5	8	0.2	2	4	80 (He)	~ 1
Tristan AR [17]	45	1000	2.5	100	0.8	2	9	120 (N_2)	0.2
PLS [18]	12	120	2	120	0.3	2	3,6	5 (He)	≤ 1
PEP-II [19]	28	2000	9	700	0.7	4.2	25,20	5	< 1 (?)
KEKB HER [20]	24	360	8	100	1.5	8	15	1	4.6
ESRF [22]	4	10	6	500	0.5	2.7	20	5	≤ 1
SPring-8 [23]	6	15	8	60	0.2	2	15	0.5	~ 2

and the chamber dimension. The secondary electrons consist of both true secondaries and elastically scattered or rediffused electrons [29, 30].

The electron build up saturates when the attractive beam field is on average compensated by the field of the electrons, and the saturated electron line density $\lambda_{\rm el}$ is roughly $\lambda_{\rm el,neutr} \approx N_b/L_{\rm sep}$, for which the electron field on average compensates the beam field at the chamber wall. This corresponds to a volume density

$$\rho_{\rm el,neutr} \approx \lambda_{\rm el,neutr}/(\pi h_x h_y) \ , \qquad (10)$$

where $(\pi h_x h_y)$ is the chamber cross section.

The electron cloud links the motion of subsequent bunches and can induce a coupled-bunch instability [3, 4], because bunches which are off-set transversely will perturb the electron-cloud distribution and, thereby, the following bunches. This instability may be cured by a fast bunch-by-bunch feedback system.

More importantly, the electron cloud also drives a single-bunch instability [5, 6]. The single-bunch wake field and the associated ECI threshold have been estimated in a variety of ways. The simplest is a two particle model [6], where the bunch consists of a head and tail particle, each carrying the charge $N_b e/2$. Unlike an ordinary wake field, a finite length, about σ_z, must be assigned to the leading particle, since the electron motion depends on the beam line density. For sufficiently long bunches, *i.e.*, $\sigma_z \omega_e > c\pi/2$, the wake field acting on the trailing particle (in units of $\rm m^{-2}$) is [6]

$$W_y \approx 8\pi\rho_e C/N_b \ . \qquad (11)$$

Note that the electron density increases roughly in proportion to the population of the (preceding) bunches, $\rho_e \propto N_b$, so that, for equally intense bunches, W_y is independent of N_b as for a regular wake field. Further assuming that the electron density equals the neutralization density (10), $\rho_{\rm e,neutr}$, the wake field (11) becomes $W_y \approx 8C/(L_{\rm sep} h_x h_y)$, which contains only geometric quantities. In a ring with synchrotron oscillations, the instability manifests itself as a strong head-tail or transverse mode-coupling instability (TMCI). Using (11) the electron density at the TMCI threshold is [6]

$$\rho_{\rm e,thr} \approx \frac{2\gamma Q_s}{\pi\beta_y \, r_p C} \ , \qquad (12)$$

where Q_s is the synchrotron tune. Since $\rho_{\rm e,neutr} \propto N_b/L_{\rm sep}$, this implies the scaling $N_{b,\rm thr} \propto L_{\rm sep}$, in agreement with some observations [31]. Table 2 illustrates that for many future or present accelerators, *e.g.*, PEP-II, KEKB, LHC, SPS, the neutralization density (10) exceeds the threshold (12) [8]. Alternative estimates can be derived from a standard mode-coupling analysis, after approximating the electron-cloud wake field by a resonator [32] $W_y(z) \approx W_0 \exp(-\alpha z)\sin(\omega_e z/c)$. The parameters W_0 and α are obtained from simulations. For a rigid Gaussian distribution of electrons whose size equals the beam size, an analytical estimate for W_0 in units of $\rm m^{-2}$ is $W_0 \approx (2\pi)^{5/4}\sigma_x\sigma_y C r_e^{1/2}/(\sigma_y^{3/2}(\sigma_x+\sigma_y)^{3/2})\sqrt{\sigma_z/N_b}$ [32]. However, the simulated value for a large non-rigid cloud is 3–20 times larger [32], which is explained by the accumulation of electrons near the beam axis during a bunch passage [33].

Beam instabilities due to electrons were first observed with coasting proton beams or long single proton bunches in Novosibirsk [34], the CERN ISR [35], and at the Los Alamos PSR [36]. Beam-induced multipacting was already seen at the ISR, in bunched beam operation [28]. The first observation of a coupled-bunch electron-cloud instabilities for a positron beam was made at the KEK Photon Factory [3, 4]. The effect was reproduced in BEPC [37]. Thereafter, studies were launched for the PEP-II B factory [38], and LHC [40]. Since 1998, electron-cloud effects are seen with the LHC proton beam in the SPS [41], and since 2000 in the CERN PS prior to beam extraction, as well as in the PS-to-SPS transfer line [42]. Electron clouds are also responsible for beam-size blow up and luminosity limitations observed in the two positron rings of PEP-II [43] and KEKB [31, 44, 45], where the simulated build up of electrons along a bunch train nicely coincided with the measured blow up [5]. In the absence of coupled bunch oscillations, it was proposed that the blow up is due to a single-bunch instability driven by the electrons [5, 6]. This has been confirmed by a witness bunch experiment [44]. Subsequent observations at the CERN SPS include beam loss and emittance growth, and evidence for coupled-bunch motion in the horizontal plane and for a single-bunch instability in the vertical. At the SPS, the vertical motion inside individual bunches was detected by a broadband pick up,

Table 2: Selected parameters for some present and future storage rings in which an electron cloud is observed or expected (PS and SPS numbers refer to the use as LHC injectors, TESLA and NLC numbers to the damping rings.)

accelerator	PEP-II	KEKB	TESLA	NLC	PS	SPS	LHC
species	e^+	e^+	e^+	e^+	p	p	p
beam energy [GeV]	3.1	3.5	5	1.98	26	26	7000
bunch population N_b [10^{10}]	9	3.3	2	1.5	11	11	11
bunch spacing $L_{\rm sep}$ [m]	2.5	2.4	6	0.84	7.5	7.5	7.5
rms bunch length σ_z [mm]	13	4	6	3.6	300	300	77
rms beam sizes $\sigma_{x,y}$ [mm]	1.4, 0.2	0.42, 0.06	0.23	0.04, 0.009	2.4, 1.3	3, 2.3	0.3, 0.3
chamber half dimensions $h_{x,y}$ [mm]	25	47	48	16	70, 35	70, 22.5	22, 18
synchrotron tune Q_s	0.03	0.015	0.1	0.0035	0.004	0.006	0.002
circumference C [km]	2.2	3.0	17	0.3	0.63	6.9	27
average beta function β	18	15	127	5	15	40	80
e^- osc./bunch $n_{\rm osc} \equiv \omega_e \sigma_z/(\pi c)$	0.9	1.0	0.5	5.2	1.2	0.78	3.3
TMCI threshold ρ_e [10^{12} m^{-3}]	1	0.5	0.1	2.1	5	0.25	3
density ratio $\rho_{\rm e,neutr}/\rho_{\rm e,thr}$	19	4	4	11	0.35	11	4

and fitted to a wake-field with a frequency of order ω_e [46].

Various simulation codes model the build up of the electron cloud in the vacuum chamber [4, 30, 39], the wake field and the single-bunch instability [6, 47, 48, 49]. Since the electron density and oscillation frequency ω_e vary along the bunch, this wake field is not time invariant and depends on the source point, different from a regular wake.

The increase in the electron density during the bunch passage causes a tune difference between bunch head and tail. For lower-energy proton beams an additional tune variation along the bunch arises from the beam space charge. Simulations suggest that adding the proton space-charge to the electron cloud qualitatively changes the character of the single-bunch instability [50].

For the LHC and any future hadron collider employing superconducting magnets, an important concern is the heat load deposited by the electron cloud on the cryogenic system. The electron energy incident on the chamber wall can exceed the heat deposited by proton synchrotron radiation (about 0.2 W/m) and the available cooling capacity; see Fig. 1. Special chamber preparations and commissioning recipes are foreseen to stay within tolerable limits. The surface conditioning, *i.e.*, the decrease of the maximum secondary emission yield $\delta_{\rm max}$ as a function of accumulated electron dose will play a central role.

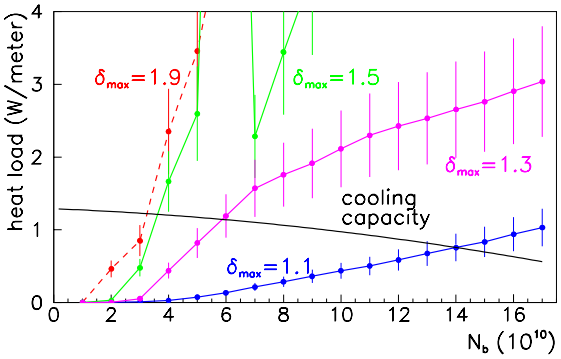

Figure 1: Simulated average LHC arc heat load and cooling capacity as a function of bunch population N_b, for various values of the maximum secondary emission yield $\delta_{\rm max}$.

4 OUTLOOK

So far the fast beam-ion instability has proven rather benign. This may be attributed to the good vacuum pressure (< 1 ntorr) achieved in most machines and to the efficiency of the bunch-by-bunch feedback systems. It may not be the case for future machines with ultra-low emittances.

At present, the effects of the electron cloud are more severe. They have limited the performance of several machines (PSR, KEK PF, B factories, LHC beam in the SPS). A variety of cures have been proposed and tested.

First, one may decrease the electron production. The generation of photo-electrons is suppressed by antechambers (PEP-II) or by sawtooth surfaces (LHC), which both absorb synchrotron radiation and reduce the photoemission inside the beam pipe. Coating the vacuum chamber with thin films of TiN (at PEP-II and PSR) or TiZrV (in the LHC warm sections) reduces the secondary electron yield. Alternatively, low secondary yields are also achieved by surface conditioning. This has been verified at the SPS [51] and will be applied at the LHC. Prior glow-discharge cleaning with N_2 or Ar may aid in this process [51]. Multipacting depends on the bunch length and filling pattern. Lower-charge 'satellite' bunches [52, 53, 54] or intense 'blow-out' bunches [55, 56] might remove electrons from the vicinity of the beam. Second, the electron flow can be modified by magnetic fields, such as weak solenoids (KEKB, PEP-II), or by clearing electrodes (ISR). Special bunch filling patterns minimize the average central electron density and optimize the luminosity (PEP-II, KEKB, LHC). Third, instability thresholds can be raised by Landau-damping octupoles (KEK PF, BEPC), by a large chromaticity (BEPC, SPS, KEKB), by linear coupling [57], by adjusting feedback phase and gain [58], by detuning the lattice, or by optimizing the bunch length.

It has also been proposed to perturb the electrons using

microwaves [59], *e.g.*, for a field amplitude of 100 kV/m at 5 GHz, the electrons are accelerated to 4×10^5 m/s. In simulations the rf field strongly increases the multipacting, which could be exploited for in-situ conditioning.

Finally, there is an attractive option for future proton colliders, such as for a luminosity (and/or energy) upgrade of the LHC [60], namely the collision of long 'superbunches' [61], reminiscent of the CERN ISR. Not only do long bunches promise much higher luminosity than short bunches, for an identical total beam-beam tune shift [62], but they also drastically reduce the arc heat load, since electrons traversing the quasi-static beam potential cannot gain any energy as they move from wall to wall. Only at the trailing edge of the bunch multipacting may still occur [63]. Figure 2 shows the simulated reduction of the heat load in an LHC dipole magnet as a function of bunch length, for constant luminosity. Table 3 compares the nominal and ultimate LHC parameters with those for hypothetical superbunch collisions in an upgraded LHC delivering a luminosity of 10^{35} cm^{-2}s^{-1}.

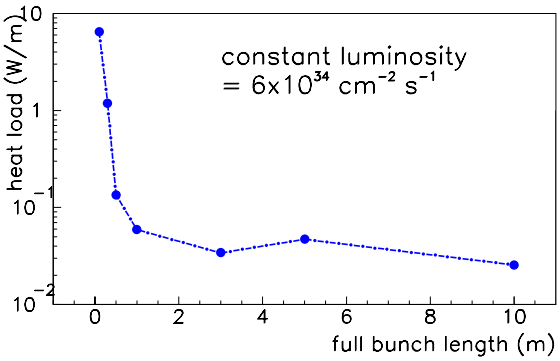

Figure 2: Simulated heat load in an LHC arc dipole due to the electron cloud as a function of superbunch length for $\delta_{\max} = 1.4$, considering a constant flat top proton line density of 8×10^{11} m^{-1} with 10% linearly rising and falling edges. The number of bunches is varied so as to keep the luminosity constant.

Table 3: Nominal and ultimate LHC parameters compared with superbunch upgrade, at 14 TeV for $\beta^*_{x,y} = 0.5$ m, $\theta_c = 300$ μrad, and $\delta_{\max} = 1.4$ (for $\delta_{\max} = 1.1$ nominal and ultimate heat loads decrease to 0.1 and 0.2 W/m).

no. of bunches	2808	2808	4
bunch population [10^{11}]	1.1	1.67	2560
bunch length ($4\sigma_z$) [m]	0.31	0.31	315
luminosity [10^{34} cm^{-2}s^{-1}]	1	2.3	10
dipole heat load [W/m]	2.0	2.2	< 0.04

5 REFERENCES

[1] T. Raubenheimer *et al.*, Phys. Rev. E 52, 5, p. 5487 (1995).
[2] G.V. Stupakov *et al.*, Phys. Rev. E 52, 5, p. 5499 (1995).
[3] M. Izawa *et al.*, Phys. Rev. Lett. 74, 5044 (1995).
[4] K. Ohmi, Phys. Rev. Lett. 75, 1526 (1995).
[5] F. Zimmermann, CERN-SL-Note-2000-004 AP (2000).
[6] K. Ohmi, F. Zimmermann, Phys. Rev. Lett. **85**, 3821 (2000).
[7] F. Zimmermann, G. Rumolo, APAC 2001, 352 (2001).
[8] F. Zimmermann, PAC 2001 Chicago, 666 (2001).
[9] G. Arduini, this conference.
[10] Workshop on Electron-Cloud Simulations, ECLOUD'02, CERN, Geneva, April 2002, CERN report CERN-2002-001, *http://slap.cern.ch/collective/ecloud02*
[11] Workshop on Two-Stream Instabilities, KEK, Tsukuba, September 2001, *http://conference.kek.jp/two-stream/*
[12] See bibliography in Ref. [8].
[13] G.V Stupakov, Proc. CEIBA'95, KEK 96-6 (1996).
[14] R.A. Bosch, PRST-AB 3, 034402 (2000).
[15] S. Heifets, IEEE PAC 97 Vancouver, 1620 (1997).
[16] J. Byrd *et al.*, Phys. Rev. Lett. 79, 79 (1997).
[17] H. Fukuma *et al.*, Proc. MBI'97, KEK 97-17, p. 1 (1997).
[18] M. Kwon *et al.*, Phys. Rev. E 57, 5, p. 6016 (1998); J Huang *et al.*, Phys. Rev. Lett. 81, p. 4388 (1998).
[19] F. Zimmermann *et al.*, Frascati Phys. S. X, p. 399 (1997).
[20] Y. Ohnishi *et al.*, Proc. EPAC2000, Vienna, p. 1167 (2000).
[21] J. Irwin *et al.*, Phys. Rev. Lett. 82, p. 1684 (1999).
[22] R. Nagaoka *et al.*, EPAC 2000 Vienna, 1158 (2000).
[23] T. Nakamura *et al.*, PAC 2001, 1966 (2001) and in Ref. [11].
[24] S.S. Win *et al.*, APAC01, 380 (2001).
[25] F. Zimmermann, Proc. MBI'97, KEK 97-17, p. 23 (1997).
[26] F. Zimmermann, SLAC-AP-107 (1997).
[27] K.Y. Ng *et al.*, in Ref. [11].
[28] O. Gröbner, HEACC'77, Protvino (1977).
[29] H. Seiler, J. Appl. Phys. 54 (11) (1983); R. Kirby *et al.*, SLAC-PUB-8212 (2000); V. Baglin *et al.*, LHC-Project-Report-472 (2001).
[30] M.A. Furman *et al.*, KEK Proc. 97-17, p. 170 (1997);
[31] K. Oide, Chamonix XI, CERN-SL-2000-007 DI (2001).
[32] K. Ohmi et al., PRE 65, 016502 (2002).
[33] M.A. Furman *et al.*, PAC99 Washington (1999).
[34] G.I. Dimov *et al.*, Soviet Conf. Charged Part. Acc., Moscow 1968, p. 312 (1968); V. Dudnikov, IEEE PAC 2001 Chicago.
[35] H. Hereward, CERN 71-15; E. Keil, B. Zotter, CERN-ISR-TH-71-58 (1971).
[36] D. Neuffer *et al.*, Part. Acc. 23 (1988); NIM A 321 (1992).
[37] Z.Y. Guo *et al.*, APAC 98, 432 (1998).
[38] S. Heifets, SLAC-PUB-6956 (1995); M. A. Furman *et al.*, PAC97, Vancouver, 1617 (1997).
[39] F. Zimmermann, LHC PR 95, SLAC-PUB-7425 (1997); G. Rumolo and F. Zimmermann, SL Note 2002-016.
[40] See *http://slap.cern.ch/collective/electron-cloud*
[41] G. Arduini *et al.*, EPAC 2000, 341; PAC 2001, 1883.
[42] E. Metral *et al.*, PAC 2001, 682 (2001).
[43] A. Fisher, HEACC'01, SLAC-PUB-8815 (2001).
[44] H. Fukuma *et al.*, HEACC'01 Tsukuba (2001); H. Fukuma *et al.*, EPAC2000, 1122 (2000); H. Fukuma and K. Ohmi, private communications (2001).
[45] T. Ieiri *et al.*, HEACC01 Tsukuba (2001).
[46] K. Cornelis, Chamonix XI, CERN-SL-2001-003-DI.
[47] G. Rumolo *et al.*, PAC 2001, Chicago, 1886 (2001); K. Ohmi, PAC 2001, Chicago, 1895 (2001).
[48] T. Katsouleas, in Ref. [10].
[49] Y. Cai *et al.*, PAC2001, and in Ref. [10].
[50] G. Rumolo *et al.*, in Ref. [11]
[51] J.M. Jimenez, CERN-SL-2001-003-DI, and in Ref. [10].
[52] F. Ruggiero *et al.*, BNL, AIP Conf. Proc. 496 (1999).
[53] B. Richter, SLAC memo, unpublished (2000).
[54] F. Zimmermann, Chamonix X & XI, CERN-SL-2000-007 & 2001-003-DI; G. Rumolo, *et al.*, PRST-AB 012801 (2001).
[55] S. Heifets, in Ref. [10].
[56] K. Oide, private communication (2002).
[57] E. Metral, in Ref. [10].
[58] E. Perevedentsev, in Ref. [10].
[59] A. Chao, private communication (1997); F. Caspers, proposal at ECLOUD'02 (2002).
[60] F. Ruggiero (ed.), "LHC Luminosity and Energy Upgrade: A Feasibility Study," LHC Project Report in preparation.
[61] K. Takayama *et al*, PRL 88, 144801 (2002).
[62] F. Ruggiero, F. Zimmermann, publ. in PRST-AB (2002).
[63] R. Macek *et al.*, PAC2001, 688; M. Furman, M. Pivi *et al.*, PAC2001, 707 (2001).